SLAC-PUB-12711
August 2007

The Distribution of Oxide Species in the Cs/O Activation Layer on InP(100) Negative Electron Affinity Photocathodes

Dong-Ick Lee

Department of Materials Science and Engineering, Stanford University, Stanford, CA 94305

Yun Sun [a)], Zhi Liu, Shiyu Sun, Samuel Peterson, and Piero Pianetta

Stanford Synchrotron Radiation Laboratory, Menlo Park, California 94025

Abstract:

The atomic arrangement of Cs oxides in the activation layer of an InP photocathode is investigated using Angle Dependent Photoemission Spectroscopy (ADPES). Two distinct peaks in the O1s core level and in valence band spectra have led to the discovery of two molecular oxygen species incorporated in the thin activation layer: Cs peroxide (Cs_2O_2) and Cs superoxide (CsO_2). The different angular dependences of these oxides observed in the photoemission spectra are caused by different vertical locations of the oxygen molecules in each Cs oxide in the activation layer. The thickness of the activation layer, which is about 7**Å**, suggests lateral distribution of Cs peroxide and Cs superoxide. The quantum efficiency (QE) of InP photocathodes in our Ultra High Vacuum (UHV) system decreases with time due to the chemical transformation of the Cs oxides and subsequent substrate oxidation, as deduced from an

[a)] ssun@slac.stanford.edu; corresponding author

Submitted to Journal of Applied Physics
Work supported in part by US Department of Energy contract DE-AC02-76SF00515

observation of the peak evolution in the photoemission spectra, and supported by the thermodynamic stability of Cs superoxide as compared to Cs peroxide when there is residual oxygen around.

I. INTRODUCTION

III-V semiconductors have been used as sensitive photocathodes after their surfaces have been converted into a negative electron affinity state. A surface is considered to have a negative electron affinity (NEA) when the vacuum level becomes lower than the bulk conduction band minimum thus allowing electrons excited across the band gap to escape into vacuum. NEA photocathodes can be used for two dimensional imaging applications in the infrared region. To achieve NEA, the photocathode is activated by co-depositing Cs and O on p-type III-V semiconductor surfaces [1]. Among the III-V semiconductors, GaAs has been the primary material used and has found wide applications in night vision imaging devices. However, InP based alloys have recently been employed in longer wavelength imaging systems which require a better understanding of the NEA characteristics of InP itself [2].

The Cs/O activation layer is critical for any photocathode to achieve high quantum efficiency (QE). Although there have been attempts to explain the phenomenon behind the vacuum level lowering by Cs/O activation [3 – 10], none of these models have successfully described the chemical species within the Cs/O activation layer. Two major questions that remain unanswered are: 1) what is the chemical composition of the Cs/O layer; and 2) what is the atomic arrangement of the atoms in this layer? Another concern for practical applications is that the Cs/O layer of an activated NEA photocathode is extremely sensitive to contamination which can

destroy the NEA properties of the surface and significantly reduce its QE [11].

In this study, we investigated the Cs/O activation layer on an InP substrate using synchrotron radiation photoemission spectroscopy (SR-PES). We were able to observe two different cesium oxides, namely Cs peroxide and Cs superoxide. Using angle-dependent photoemission spectroscopy (ADPES), we discovered that the Cs peroxide and superoxide were distributed laterally in the activation layer. Furthermore, we found that the decay of the QE is due to the transformation of the Cs peroxides into the Cs superoxides and the subsequent oxidation of the substrate. These changes are consistent with our simple lateral distribution model and they are the consequences of the thermal stability of Cs superoxides compared to Cs peroxides at room temperature when residual oxygen is present.

II. EXPERIMENT

The samples used in this study were Zn doped p-type InP(100) crystals provided by *Wafer Technology, UK*, with doping concentrations of 5×10^{17} cm^{-3}, and a wafer thickness of 0.35 mm. To clean the InP(100) surface, we used the two-step cleaning process described in [12]. All the chemical cleaning was performed in a glove bag which had an Ar-purged environment.

The activation process involves depositing 0.5 ML of Cs first followed by alternating steps of Cs+O co-deposition and Cs alone deposition, which is described in detail in [2]. Cesium

was evaporated from a SAES Cs getter chromate source. This Cs getter was carefully out-gassed before use as described in reference [13]. Molecular oxygen was introduced into the chamber through a leak valve. Ion gauge was turned off during activation because ionized oxygen contributes to the accelerated oxidation of III-V semiconductors, which is not desired in this study [14]. The pressure was measured using the ion pump current which was previously calibrated using an ion gauge. During the co-deposition of Cs and O, sample was held at room temperature. A He-Ne laser (632.8nm) was used to generate photoelectrons to monitor the activation process. To calculate QE, the number of photoelectrons collected is divided by the number of photons, which is measured by a calibrated Si photodiode.

For angular dependent photoelectron spectroscopy, we changed the emission angle by rotating the sample with respect to the analyzer, which change the surface sensitivity. Figure 1 shows two extreme configurations. In the configuration with a 90^{o} emission angle, the probing depth was maximized at a given photon energy (relatively bulk-sensitive), while the probing depth became smaller in the configuration with a 30^{o} emission angle (relatively surface-sensitive).

III. RESULTS AND DISCUSSIONS

A. Angle-dependent photoemission measurements

It is discovered in our earlier studies that there are two types of Cs oxides in the

activation layer after the InP is activated by Cs and oxygen [15], where the identification of Cs peroxide and superoxide is based on comparing the valence band spectra of our activated InP photocathode with the well established literature of oxidation of bulk Cs [16-23]. The valence band spectra of the activated InP are shown in figure 2 (a). Peak A (with kinetic energy of 62.5 eV) is related to the peroxide Cs_2O_2, while peaks B (with kinetic energy of 60.7 eV) and C (with kinetic energy of 56.9 eV) are related to the superoxide CsO_2. The O1s spectrum is shown in Figure 3, and two types of oxygen species are clearly seen. Peak A, with kinetic energy of 103.3 eV, is assigned as the oxygen in the peroxide, and peak B, with kinetic energy of 100.8 eV, is assigned as the oxygen in the superoxide, since peroxide ion is electron richer than superoxide ion.

The angular dependence of the O1s intensities in the cesium oxides is also shown in figure 3. When the emission angle becomes larger, the relative intensity of peak A (Cs peroxide) becomes larger, while the relative intensity of peak B (Cs superoxide) becomes smaller. This result implies that the oxygen in the cesium peroxide is located deeper in the Cs/O activation layer, while that of the cesium superoxide is nearer to the surface, because photoemission with the 90^o emission angle is relatively bulk-sensitive and photoemission with the 30^o emission angle is relatively surface-sensitive. The three main peaks in the valence band spectra shown in Figure 2 have angular dependence similar to the peaks in the O1s core level spectra. Immediately after

activation (Figure 2(a)), peak A (cesium peroxide) exhibits higher intensity at the 90^{o} emission angle than at the 30^{o} emission angle, while peak B and peak C (cesium superoxide) exhibit lower intensity at the 90^{o} emission angle than at 30^{o}.

The QE of an activated InP photocathode decays in our vacuum system, accompanied by changes in both the O1s and VB spectra [15]. In short, peaks related to superoxides grow, while peaks related to peroxides become smaller over time and, at the same time, substrate oxidation mainly on In sites occurs. The angular dependence of the O1s and VB spectra were tracked during this decay process. For the O1s spectra, we found that the original angular dependence was maintained during decay, as was the angular dependence of the VB spectra in the early stage of the decay. In the later stages of the decay, peaks A and B in the VB still maintained the angular dependence mentioned earlier. Peak C, however, reversed its angular dependence (Figure 2(d)). This is because peak C has two contributions at the later stage of decay: the cesium superoxide and the O2p bonding orbital of the substrate oxide, which cannot be resolved due to the closeness of the peak positions. Since the substrate oxide is formed on the substrate, and the Cs oxide layer is on top of it, substrate oxides are located deeper than both Cs superoxides and Cs peroxides. Therefore, it is relatively large at normal emission compared with glancing emission angles, exactly the opposite to the Cs superoxides. At the beginning of the decay (i.e. Figures 2(a) and (b)), the contribution of the oxygen intensity from the substrate oxide is very small, so

that the angular dependence of peak C is largely due to the characteristics of the Cs superoxide component. As the decay proceeds, the InP substrate is more oxidized [2], the contribution from the substrate oxide leads to the reversed angular dependence of peak C, shown in Figure 2(d).

B. Lateral distribution model of Cs/O layer and calculation of relative intensities of O1s

Figure 4 illustrates a simplified model of cesium peroxide and superoxide in the activation layer on an activated InP(100) photocathode. The model is based upon the structure of bulk Cs peroxide and superoxide [24], and captures the ratio between Cs and O for peroxide ($Cs:O_2^{2-}$ = 2:1) and superoxide ($Cs:O_2^{-}$ = 1:1). These two Cs oxide species are found to be laterally distributed, instead of being vertically stacked, because of the thickness of the Cs/O layer is small. We estimated the total thickness of the activation layer (t) from the attenuation of the In4d core level intensity by the Cs/O layer, which is 7 +/- 2 **Å**. If Cs peroxide and Cs superoxide are stacked vertically, the minimum thickness of the Cs/O will be around 14 **Å,** well over the thickness observed in our study. However, it is not intuitive that the lateral distribution of Cs peroxide and Cs superoxide will result in the angular dependence we observed in the O1s as well as in the valence band spectra because that data seem to imply that oxygen Cs peroxide is located deeper. We need to carry out a simple mathematical modeling to see if the lateral distribution is consistent with the observed angular dependence.

Because of the structural differences, the angular dependence of the oxygen intensity in Cs peroxide is different from that in Cs superoxide, as reflected in Equations (1) and (2), where I_p is the total intensity of O1s peak of the peroxide, and I_s is the total intensity of O1s peak of the superoxide; *A* is a common coefficient, which includes parameters such as the cross-section, photon beam intensity, etc.; X_p and X_s are the coverage of cesium peroxide and superoxide; θ is the emission angle; and t is the total thickness of a Cs/O layer. In Equation (1), the oxygen in the Cs peroxide is attenuated by t/2, half of the Cs/O layer thickness. In Equation (2), the first term is the oxygen in the bottom layer of the Cs superoxide, which is attenuated by t, the thickness of the whole Cs/O layer; whereas the second term is the oxygen in the top layer of the Cs superoxide, which is not attenuated.

$$I_p = A \bullet X_p e^{-t/2\lambda \sin\theta} \tag{1}$$

$$I_s = A \bullet X_s e^{-t/\lambda \sin\theta} + A \bullet X_s \tag{2}$$

Based these equations and given parameters, we performed least squares fitting of the experimental data of the ratio I_p/I_s as shown in Equation (3).

$$\frac{I_p}{I_s} = \frac{X_p e^{-7/10\sin\theta}}{X_s e^{-7/5\sin\theta} + X_s} \tag{3}$$

The result of the fitting yields 2.71 as the ratio of X_p/X_s ($X_p + X_s = 1$). Based upon this

result, theoretical relative intensities were calculated and compared with the experimental data, as shown in Figure 5. The calculated values and the experimental data agree with each other fairly well. Some discrepancies between the two, which might be due to the simplicity of the lateral distribution model, the approximation of the attenuation using Equations (2) and (3), and the surface roughness, which can affect the uniformity of the Cs/O layer. In addition, there may be some chemical or physical deviations from a well-defined Cs_2O_2 and CsO_2 structure because of the thinness of the Cs/O layer. Given the simplicity of our model, the lateral distribution does successfully explains the observed angular dependence of O1s intensity in Cs peroxide and Cs superoxide.

C. Decay mechanism of Cs/O activated InP(100) photocathode

After the sample is activated, the photocurrent starts to decrease, and the decay rate is different with different chamber pressures. Two typical QE decay curves are presented in Figure 6. The decay rate with a chamber pressure at 2×10^{-10} Torr is significantly slower than at 8×10^{-10} Torr, which indicates that the amount of residual oxygen in the chamber is one of the factors that determine the decay rate since the total amount of oxygen in the Cs/O activation layer increases during decay [15].

This QE decay is due to the chemical changes in the Cs/O activation layer as evidenced

by the photoemission spectra of the O1s core level and the valence band in Figure 7, and by the oxidation of the InP substrate [15]. As shown in Figure 7(a), the higher kinetic energy peak (peroxide peak) decreases in intensity with time, while the lower kinetic energy peak (superoxide peak) increases in intensity. This change in intensities of the two peaks is also apparent in the valence band spectra at different times after activation (Figure 7(b)); the peroxide peak decreases and the superoxide peak increases. In addition, InP substrate oxidation is also observe during the decay [15].

Figure 8 illustrates the decay steps of a Cs/O layer, based upon the simplified structural model presented above. Early in decay, the residual oxygen molecules approach the surface of the Cs/O layer, as shown in Figure 8(a). As the residual oxygen molecules come onto the activation layer, Cs peroxide is turned into Cs superoxide, as shown in Figure 8(b) and (c). Some oxygen molecules in the bottom layer of the activation layer are dissociated and oxidize the substrate, as shown in Figure 8(d). This dissociation of O_2^{2-} is facilitated by the filling of the anti-bonding orbital of O_2 [2].

This transformation from Cs peroxide to Cs superoxide is thermodynamically favorable since Cs superoxides are more stable than Cs peroxides at room temperature, as shown in Equation (4).

$$Cs_2O_2 + O_2 \Rightarrow 2CsO_2 \qquad \Delta G = -229.8 KJ/mol \qquad (4)$$

If the reaction of Equation (4) occurs in the Cs/O layer, then we should expect that the decrease in the Cs peroxide coverage to be matched by the increase in the Cs superoxide coverage. The coverage change in Cs superoxides and peroxides can be expressed in terms of oxygen intensities in the O1s core level spectra, as shown in Equations (5) and (6), based upon our lateral distribution model.

$$\Delta X_s = C * I_s * (1 + e^{-2a/\lambda})^{-1} - X_s^0 \qquad (5)$$

$$\Delta X_p = C * I_p * e^{a/\lambda} - X_p^0 \qquad (6)$$

We have compared the coverage decrease of the Cs peroxide ($-\Delta X_p$) versus the the coverage increase of the Cs superoxide (ΔX_s), as shown in Figure 9. The increase in Cs superoxide coverage is in reasonable agreement with the decrease of Cs peroxide coverage. However, there is a small discrepancy between ΔX_s and $-\Delta X_p$ in Figure 9 at later stage of the decay. This can be explained by the growth of substrate oxide. The O1s component due to the substrate oxide is very close to the superoxide peak, so this substrate oxide contribution will make the 'superoxide' peak seems larger than it should be, thus resulting in the discrepancy.

IV. CONCLUSIONS

A very thin Cs/O layer (7 +/- 2 **Å**) was observed on the activated surface of the InP(100) photocathode. We identified two different kinds of cesium oxide after activation of InP: cesium peroxide and cesium superoxide. Oxygen molecules in the peroxide and superoxide displayed different angular dependences in both the valence band spectra and O1s core level spectra, which led us to propose a simple lateral distribution model of cesium superoxide and cesium peroxide. The expected angular dependence based on the lateral distribution of peroxide and superoxide matches well with the ADPES O1s core level data. The decay of QE is caused by the chemical transformation from Cs peroxide to Cs superoxide, and subsequent substrate oxidation. Cs superoxides are thermally more stable than Cs peroxides with residual oxygen present, and the Cs superoxides tend to dissociate to oxidize the substrate due to the filling of anti-bonding orbital of O_2. The reaction of Cs oxide transformation is consistent with the change of Cs peroxide and Cs superoxide coverage calculated based on the simple lateral distribution model.

ACKNOWLEDGEMENTS

This work was performed under Army Contract DAAD19-02-1-0396. This study was carried out at the Stanford Synchrotron Radiation Laboratory (SSRL), a national user facility operated by Stanford University on behalf of the U.S. Department of Energy, Office of Basic Energy Sciences. Authors are grateful to the SSRL staff for their support. Most of all, authors are

sincerely grateful to Dr. William E. Spicer for all the fruitful discussions and priceless advice.

References

[1]R. L. Bell, *Negative Electron Affinity Devices*, Clarendon, Oxford (1973)

[2]Y. Sun, *Ph.D. Dissertation*, Stanford University (2003)

[3]A. H. Sommer, H. H. Whitaker, B. F. Williams, Appl. Phys. Lett. **17**, 273 (1970)

[4]B. F. Williams, J. J. Tietjen, Proc. IEEE **59**, 1489 (1971)

[5]D. G. Fisher, R. E. Enstrom, J. S. Esher, B. F. Williams, J. Appl. Phys. **43**, 3815 (1972)

[6]C. Y. Su, W. E. Spicer, I. Lindau, J. Appl. Phys. **54**, 1413 (1983)

[7]H. Sonnenberg, Appl. Phys. Lett. **14**, 289 (1969)

[8]J. J. Uebbing, L. W. James, J. Appl. Phys. **42**, 5095 (1971)

[9]W. E. Spicer, Appl. Phys. **12**, 115 (1977)

[10]M. G. Burt, V. Heine, J. Phys. C, **11**, 961 (1978)

[11]P. Sen, D. S. Pickard, J. E. Schneider, M. A. McCord, R. F. W. Pease, A. W. Baum, K. A. Costello, J. Vac. Sci. Technol. B **16**, 3380 (1998)

[12]Y. Sun, Z. Liu, F. Machuca, P. Pianetta, W. E. Spicer, J. Vac. Sci. Technol. A **21**, 219 (2003)

[13]P. Pianetta, *In Situ Processing by Gas or Alkali Metal Dosing and by Cleavage*, chapter of the book *Specimen Handling, Preparation, and Treatments in Surface Characterization*, edited by Czanderna et al. Kluwer Academic / Plenum Publishers, New York, (1998)

[14]P. Pianetta, I. Lindau, C. M. Garner, W. E. Spicer, Phys. Rev. B **18**, 2792 (1978)

[15] Y. Sun, Z. Liu and D. Lee, P. Pianetta, unpublished

[16]B. Woratschek, W. Sesselmann, J. Kuppers, G. Ertl, J. Chem. Phys, **86**, 2411 (1987)

[17]J. Jupille, P. Dolle, M. Besancon, Surf. Sci. **260**, 271 (1992)

[18]P. Dolle, M. Tommasini, J. Jupille, Surf. Sci. **211/212**, 904 (1989)

[19]E. Bertel, F. P. Netzer, G. Rosina, H. Saalfeld, Phys. Rev. B, **39**, 6082 (1989)

[20]G. Ebbinghaus, W. Braun, A. Simon, Phys. Rev. Lett. **37**, 1770 (1976)

[21]A. Simon, J. Sol. Stat. Chem. **27**, 87 (1979)

[22]G. Ebbinghaus, A. Simon, Chem. Phys. **43**, 117 (1970)

[23]F. Machuca, Z.Liu, Y. Sun, P. Pianetta, W. E. Spicer, R. F. W. Pease, J. Vac. Sci. Technol. B, **21**, 1863 (2003)

[24]M. Pedio, M. Benfatto, S. Aminpirooz, J. Haase, Phys. Rev. B, **50**, 6596 (1994)

Figure Captions

Figure 1. Sample configurations with respect to the analyzer. In configuration (a), the probing depth is maximized to deliver relatively bulk sensitive information, while in configuration (b), the probing depth is small so the information is more surface sensitive.

Figure 2. ADPES valence band spectra at hν = 70 eV (thick line: 90^o emission angle, thin line: 30^o emission angle) at different times after activation. (a) 5 minutes (b) 70 minutes (c) 148 minutes (d) 424 minutes after activation

Figure 3. O1s core level spectra at hν = 640 eV. Spectra are taken at four different emission angles. The 90^o emission angle is the most bulk sensitive, while the 30^o emission angle is the most surface sensitive.

Figure 4. Lateral distribution model of cesium superoxides and peroxides on the activated surface of an InP(100) photocathode. The total thickness of the activation layer (t) is ~7A.

Figure 5. (a) Relative intensity of peroxide ($I_s/(I_s+I_p)$) as a function of the emission angle and (b) Relative intensity of superoxide ($I_s/(I_s+I_p)$) as a function of the emission angle

Figure 6. Decrease of the quantum efficiency with time at different chamber pressures

Figure 7. Photoemission spectra of an activated InP(100) sample at different times after activation. (a) O1s core level spectra at hν = 640 eV (b) valence band spectra at hν = 70 eV

Figure 8. Schematic diagram of the transformation of the Cs oxides in the Cs/O layer based on the simplified structural model. (a) Residual oxygen molecule from the chamber approach the activation layer; (b) and (c) Cs peroxide changes to Cs superoxide (d) the oxygen molecule in the second layer of the Cs dissociates and oxidizes the InP substrate.

Figure 9. The increase of the coverage of the Cs superoxide (ΔX_s) and the decease of the coverage of the Cs peroxide ($-\Delta X_p$) were plotted as function of time during decay.

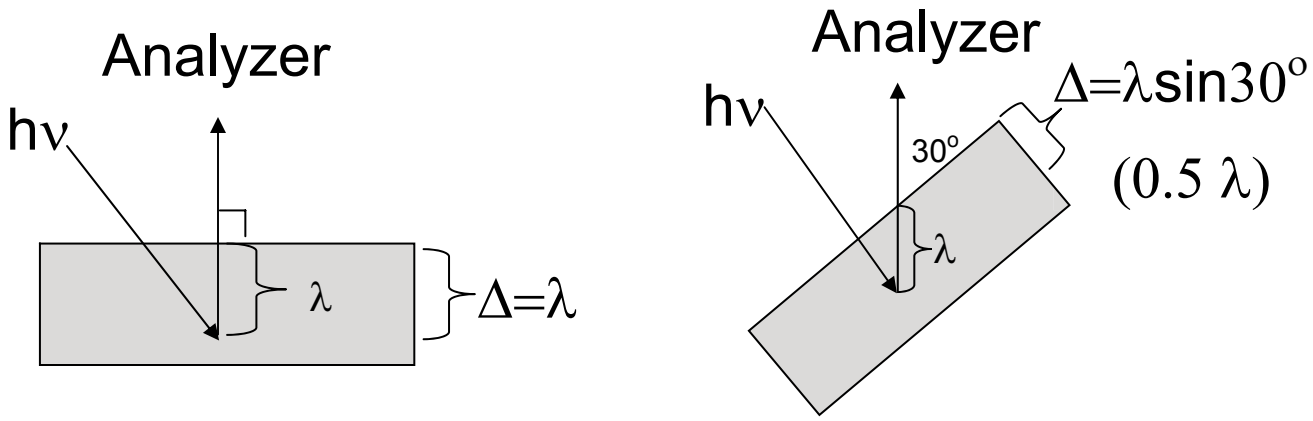

(a) 90° emission angle (b) 30° emission angle

λ: Inelastic Mean Free Path (IMPF) Δ: Probing Depth

Fig. 1

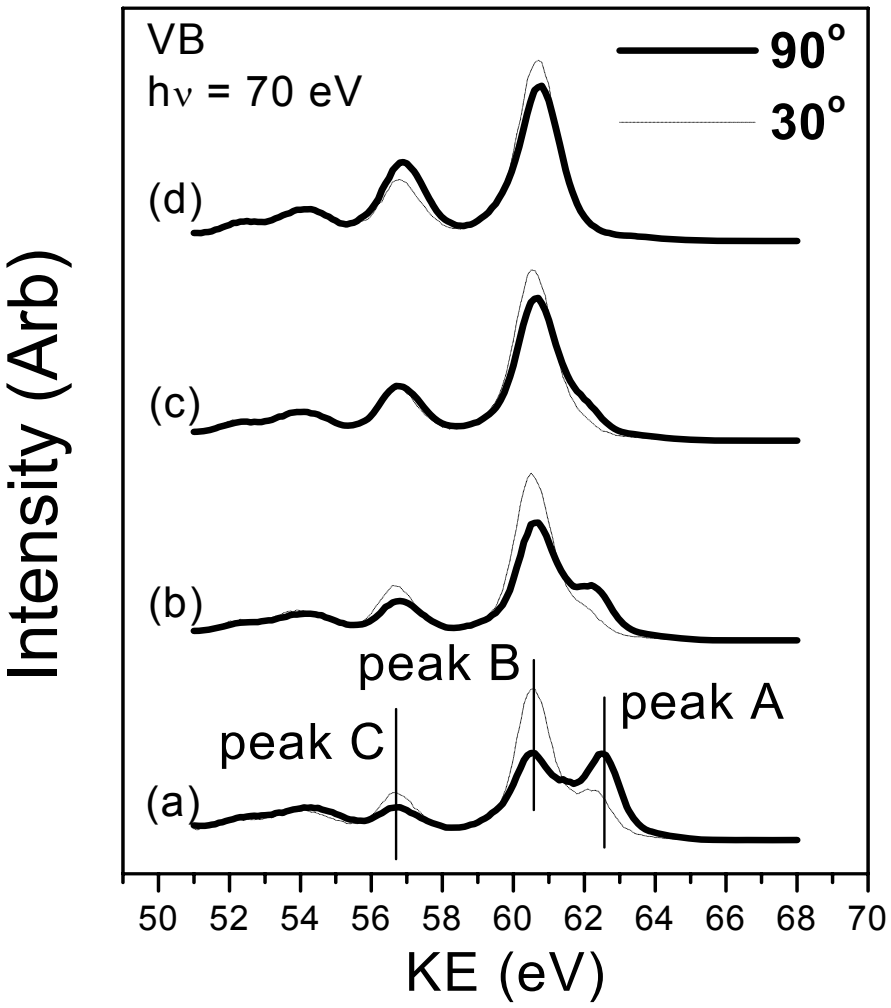
VB
hν = 70 eV
90°
30°
(d)
(c)
(b)
(a)
peak B
peak A
peak C
Intensity (Arb)
50 52 54 56 58 60 62 64 66 68 70
KE (eV)

Fig. 2

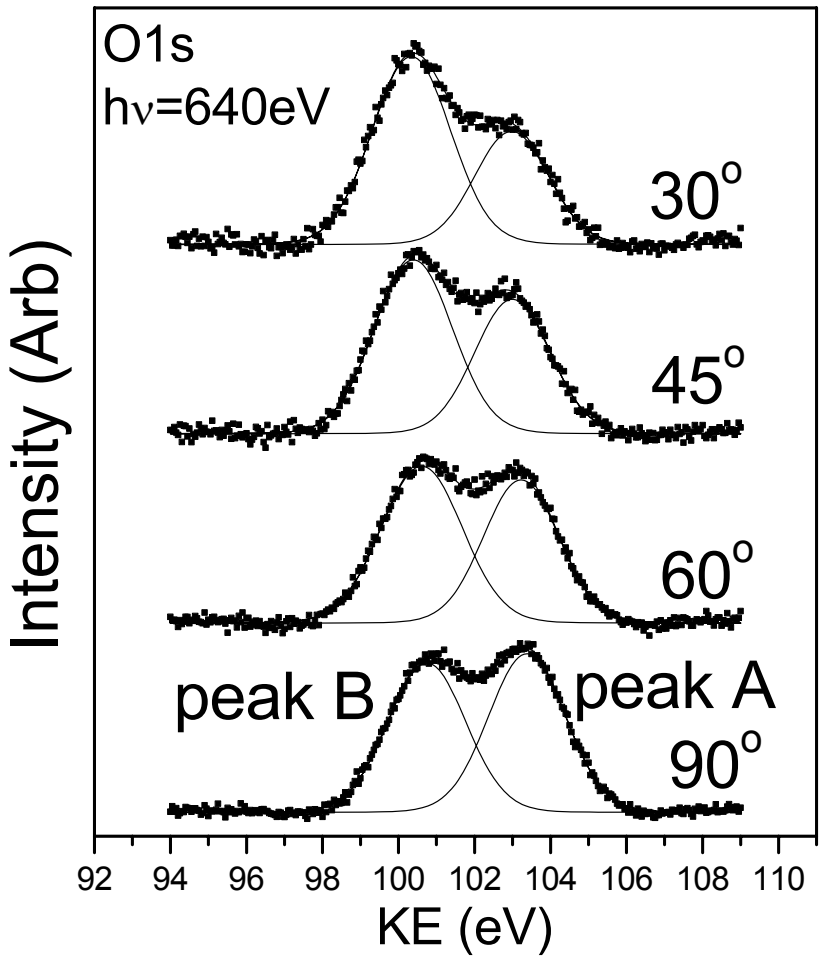
O1s
hν=640eV
30°
45°
60°
peak B
peak A
90°
Intensity (Arb)
92
94
96
98
100
102
104
106
108
110
KE (eV)

Fig. 3

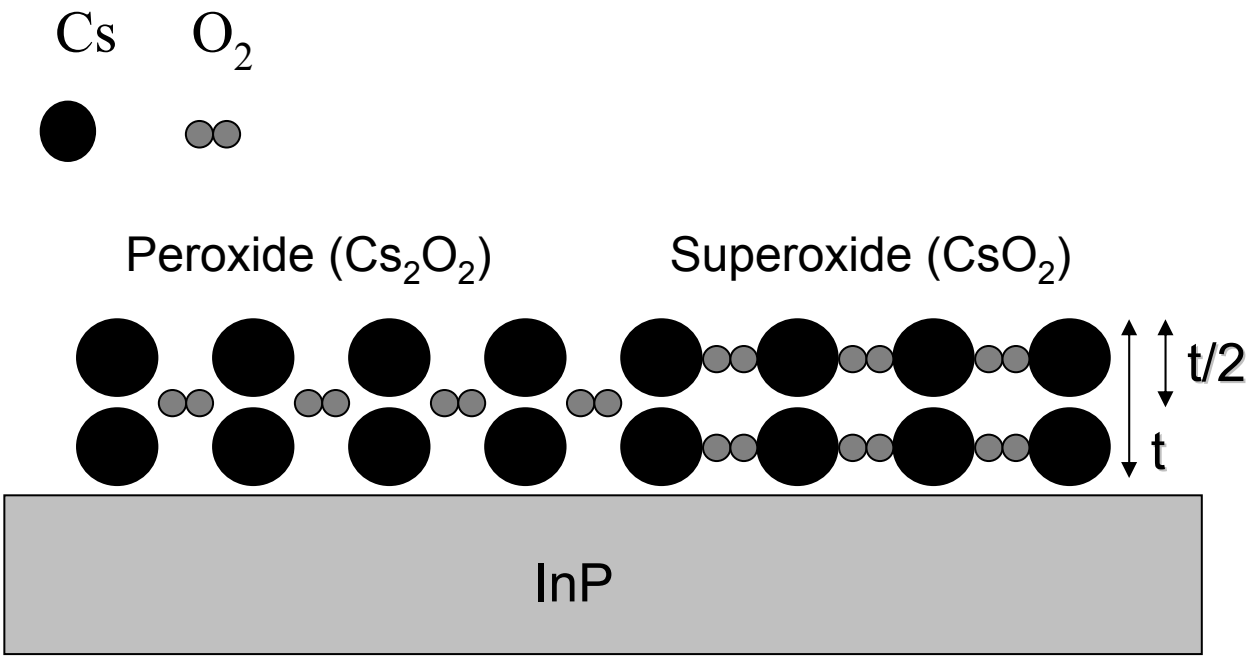

Fig. 4

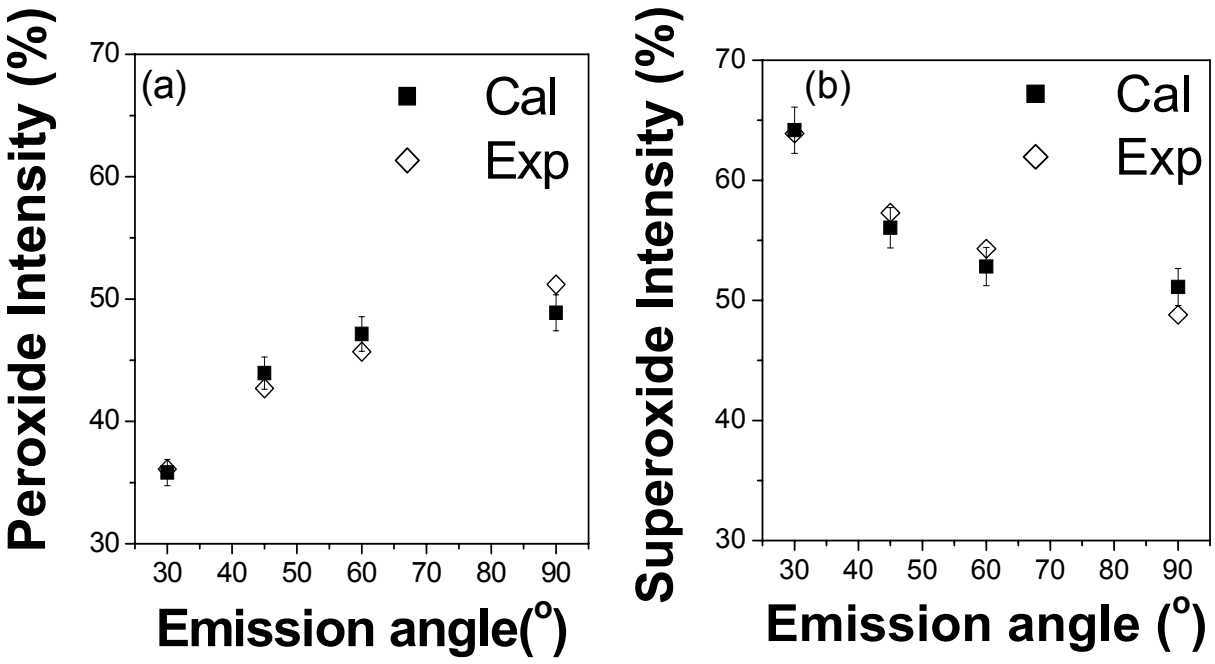
(a)
Cal
Exp
Peroxide Intensity (%)
Emission angle(°)
70
60
50
40
30
30 40 50 60 70 80 90
(b)
Cal
Exp
Superoxide Intensity (%)
Emission angle (°)
70
60
50
40
30
30 40 50 60 70 80 90

Fig. 5

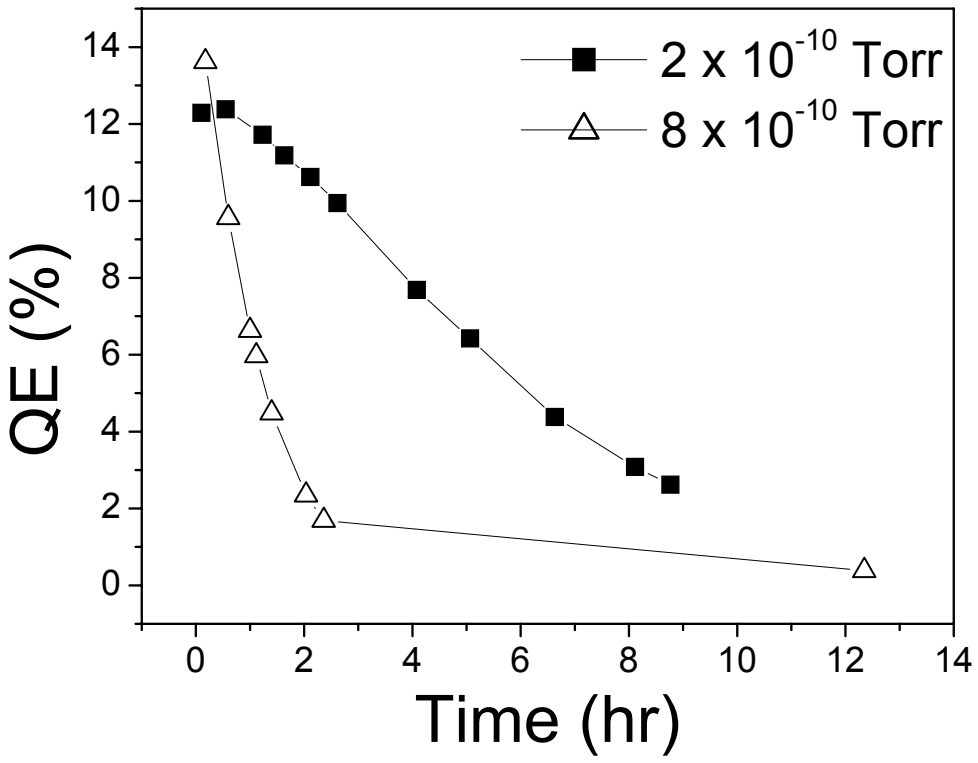

Fig. 6

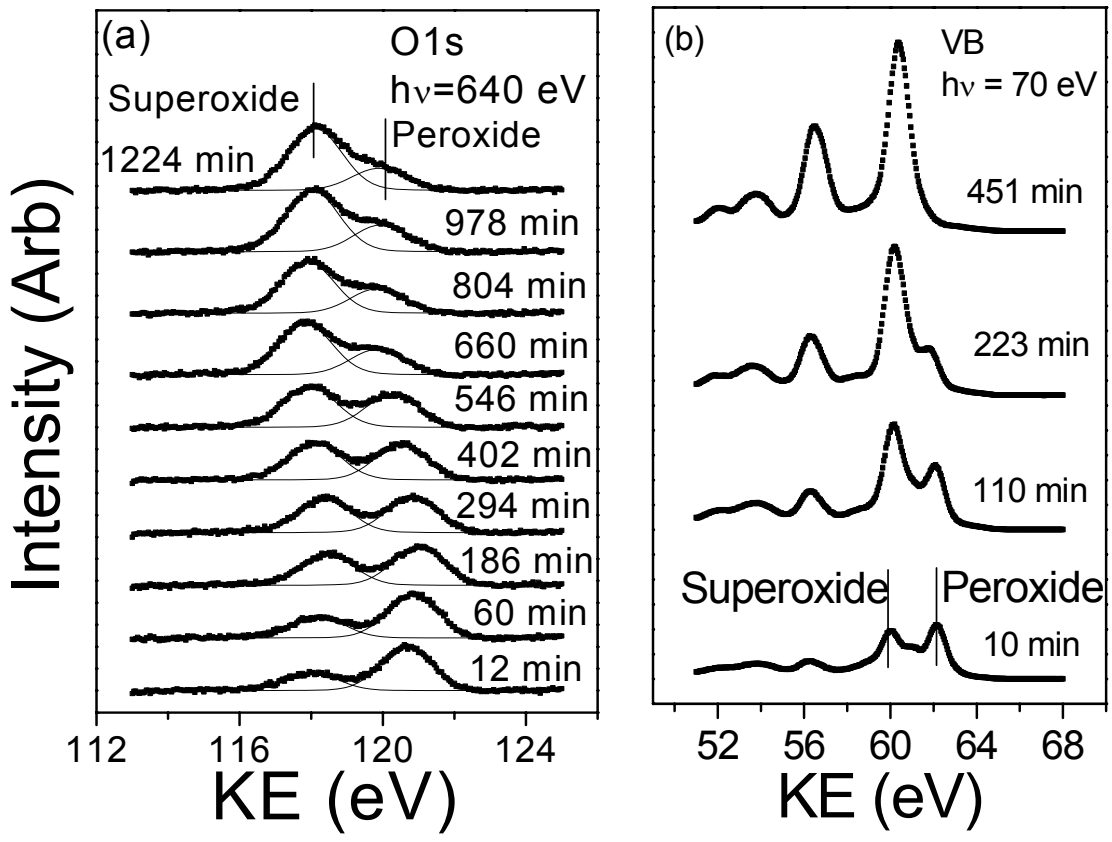
(a)
O1s
hν=640 eV
Superoxide
Peroxide
1224 min
978 min
804 min
660 min
546 min
402 min
294 min
186 min
60 min
12 min
Intensity (Arb)
112
116
120
124
KE (eV)
(b)
VB
hν = 70 eV
451 min
223 min
110 min
Superoxide
Peroxide
10 min
52
56
60
64
68
KE (eV)

Fig. 7

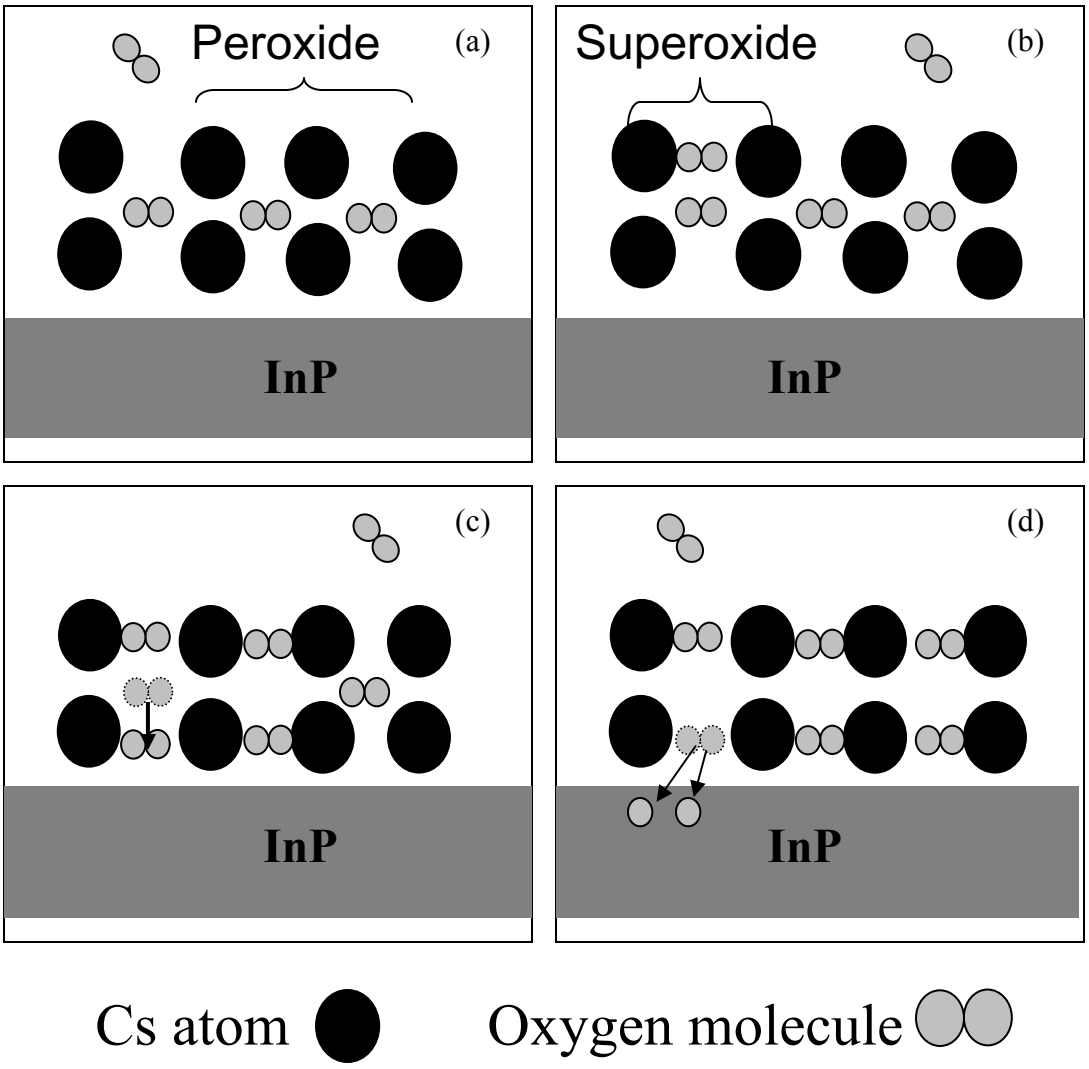
Peroxide
(a)
Superoxide
(b)
InP
InP
(c)
(d)
InP
InP
Cs atom
Oxygen molecule

Fig. 8

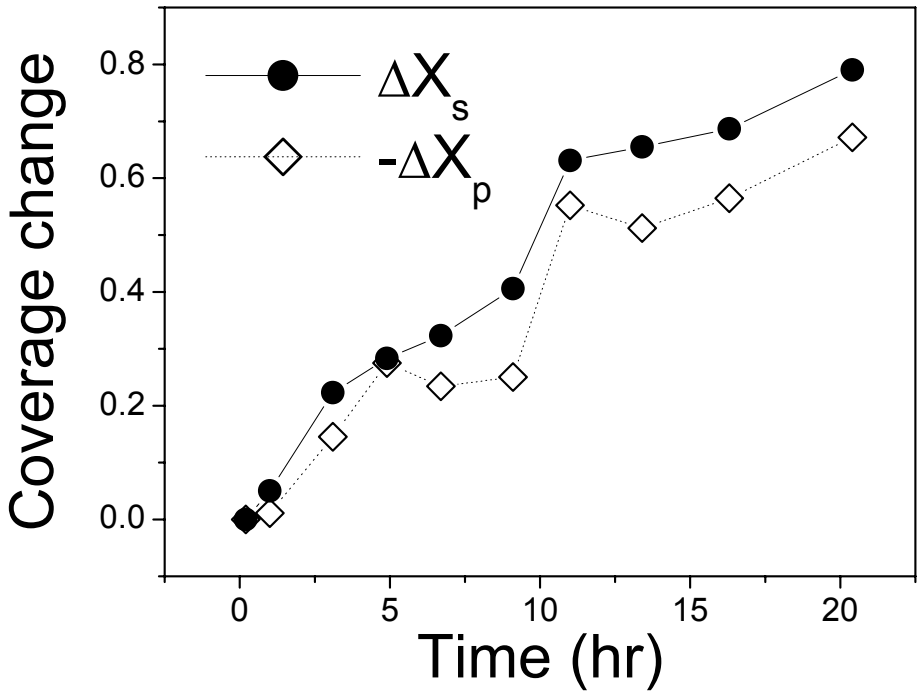

Fig. 9